Taylor & Francis
Taylor & Francis Group

Canadian Journal of Remote Sensing
Journal canadien de télédétection

ISSN: (Print) (Online) Journal homepage: www.tandfonline.com/journals/ujrs20

The WIPI Model Based on Multi-Scale Local Contrast Post-Processing for Infrared Small Target Detection

Juan Chen, Lin Qiu, Zhencai Zhu, Ning Sun, Hao Huang, Wai-Hung Ip & Kai-Leung Yung

To cite this article: Juan Chen, Lin Qiu, Zhencai Zhu, Ning Sun, Hao Huang, Wai-Hung Ip & Kai-Leung Yung (2024) The WIPI Model Based on Multi-Scale Local Contrast Post-Processing for Infrared Small Target Detection, Canadian Journal of Remote Sensing, 50:1, 2305913, DOI: 10.1080/07038992.2024.2305913

To link to this article: https://doi.org/10.1080/07038992.2024.2305913

© 2024 The Author(s). Published by Informa UK Limited, trading as Taylor & Francis Group.

Published online: 05 Mar 2024.

Submit your article to this journal

Article views: 455

View related articles

View Crossmark data

Full Terms & Conditions of access and use can be found at
https://www.tandfonline.com/action/journalInformation?journalCode=ujrs20

CANADIAN JOURNAL OF REMOTE SENSING
2024, VOL. 50, NO. 1, 2305913
https://doi.org/10.1080/07038992.2024.2305913

Taylor & Francis
Taylor & Francis Group

OPEN ACCESS Check for updates

The WIPI Model Based on Multi-Scale Local Contrast Post-Processing for Infrared Small Target Detection

Le modèle WIPI basé sur le post-traitement du contraste local multi-échelle pour la détection de petites cibles sur des images infrarouges

Juan Chen[a], Lin Qiu[a], Zhencai Zhu[a], Ning Sun[a], Hao Huang[b], Wai-Hung Ip[c,d], and Kai-Leung Yung[c]

[a]Innovation Academy for Microsatellites of CAS, University of Chinese Academy of Sciences, Shanghai, China; [b]Hubei Key Lab of Ferro & Piezoelectric Materials and Devices, Faculty of Physics and Electronic Science, Hubei University, Wuhan, China; [c]Department of Industrial and Systems Engineering, The Hong Kong Polytechnic University, Kowloon, Hong Kong, China; [d]School of Engineering, University of Saskatechewan, Saskatoon, Saskatchewan, Canada

ABSTRACT

According to the infrared patch image (IPI) model theory, the infrared image background has a low rank and the target is sparse. The low-rank model can be used to separate the background and identify the target. However, in a noisy environment, the recognition effect will be affected. The higher the noise, the harder it would be to detect a small target. The residual strong fault and background edges could reduce the detection rate and increase false alarms. The traditional IPI model is adaptable to the background with the lower noise. This paper combines weighted nuclear norm minimization (WNNM) optimization with sparse representation based on the local IPI model. The background details are described more prominently by improving the nuclear norm weighting factor. The target is much easier to detect under the specific bright clouds and ground buildings background with high noise. At the same time, post-processing with image local contrast analysis is performed to compare traditional spatial filtering and local infrared patch image model algorithms. Our method has a good suppression effect on complex noise backgrounds and achieves a higher signal to clutter ratio gain (SCRG). It could also improve the target detection rate and reduce false alarms.

RÉSUMÉ

Selon la théorie du modèle de correction des images infrarouges (IPI), l'arrière-plan de l'image infrarouge a un rang faible et la cible est clairsemée. Le modèle du rang inférieur peut être utilisé pour séparer l'arrière-plan et reconnaître la cible. Cependant, dans un environnement bruité, la reconnaissance de la cible sera affectée. Plus l'arrière-plan est bruité, plus il sera difficile de détecter une petite cible. Les erreurs résiduelles importantes et les bords d'arrière-plan peuvent réduire le taux de détection et augmenter les fausses alarmes. Le modèle IPI traditionnel est adaptable à un arrière-plan moins bruité. Cet article combine l'optimisation de la minimisation pondérée des normes nucléaires (WNNM) avec une représentation parcimonieuse basée sur le modèle local de l'IPI. Les détails de l'arrière-plan sont décrits de manière plus évidente en améliorant le facteur de pondération de la norme nucléaire. La cible est beaucoup plus facile à détecter sous des nuages lumineux et un fond de bâtiments bruité. Dans le même temps, un post-traitement avec une analyse du contraste local de l'image est effectué pour comparer les algorithmes traditionnels de filtrage spatial et notre modèle de correction des images infrarouges. Notre méthode a un bon effet de suppression sur les bruits de fond complexes et permet d'obtenir un rapport signal/bruit plus élevé. Elle pourrait également améliorer le taux de détection de la cible et réduire les fausses alarmes.

ARTICLE HISTORY
Received 9 June 2023
Accepted 9 January 2024

CONTACT Juan Chen chenjuanwentian@163.com.

© 2024 The Author(s). Published by Informa UK Limited, trading as Taylor & Francis Group.
This is an Open Access article distributed under the terms of the Creative Commons Attribution License (http://creativecommons.org/licenses/by/4.0/), which permits unrestricted use, distribution, and reproduction in any medium, provided the original work is properly cited. The terms on which this article has been published allow the posting of the Accepted Manuscript in a repository by the author(s) or with their consent.

Introduction

Infrared small target detection has been widely used in a variety of applications, including early warning and guidance systems. In an infrared detection system, small target detection is more important. Because of farther detection distance, targets usually occupy just fewer pixels in the Infrared image (Wu 2008). It usually lacks shape and texture. Due to the influence of meteorological conditions such as atmospheric refraction and scattering, the target has very weak intensity. The contrast between the target and the background is very low. It is hard to detect infrared small targets precisely. As a result, infrared small target detection has been a difficult problem for a long time.

Traditional infrared small-target detection mainly aims at detecting small cooperative targets. When the signal-to-noise ratio (SCR) is high, detection before tracking is adopted. If the SCR of the target is relatively low, tracking before detecting is adopted. Traditional small target detection algorithms include four types, spatial filtering, frequency domain filtering, contrast-based detection, and low-rank sparse detection. Spatial filtering contains max-median filtering, max-mean filtering, gaussian filtering, morphological filtering methods, etc. Frequency domain filtering mainly includes wavelet transform algorithms and low-pass filtering algorithms (Lin 2012). Spatial filtering has a high timeliness and has been widely used in the engineering practice of infrared target detection. Max-median filtering, max-mean filtering, and morphological filtering can achieve highly reliable target detection under certain specific backgrounds and specific targets, but they are highly dependent on template size. They are poor robustness to non-cooperative small target detection. They are very sensitive to high noise, which usually leads to a high false alarm rate (Jia et al. 2019).

Researchers proposed an algorithm for detecting small targets based on local contrast measurement (LCM) (Chen, et al. 2014), which can improve the accuracy of small target detection. But it causes excessive enhancement of high brightness point noise, resulting in a high false alarm rate. To solve the shortcoming of LCM, researchers have proposed an improved local contrast measurement algorithm (ILCM). It reduces false alarms. However, the robustness is low due to excessive reliance on the sliding window (Han et al. 2014). The article proposes a new LCM algorithm using a DOG filter (NLCM), which has stronger robustness in complex backgrounds and bright noise (Qin and Li 2016). However, it is prone to false alarms. Reference (Shi et al. 2017) proposes an infrared target detection algorithm based on a High boost-based multi-scale local contrast measure (HB-MLCM). The article (Han et al. 2018) proposes a multi-scale relative local contrast (RLCM). Author (Wei et al. 2016) has proposed a small target detection algorithm based on multi-scale patch contrast measurement (MPCM). Without prior knowledge, these methods improve the performance of small target detection. But they cannot adaptively select segmentation thresholds, resulting in a high false alarm rate. Many methods based on the deep learning network have been constructed to improve the accuracy of object detection on high-resolution images or hyperspectrum images, which could achieve the comprehensive feature (Ruhan et al. 2021; Yilong and Lv 2022; Cao et al. 2021; Mu et al. 2021; Lv and Li 2022). These articles have improved attention mechanism and multi-scale fusion for small target detection, multi-target and mixed-target detections (Cheng et al. 2022; Wang et al. 2023a, 2023b). However, they are not suitable for infrared data sets.

Recently, sparse representation has become widely used in target detection in complex environments. The sparse representation detection algorithm mainly utilizes the strong correlation of image frames and the sparsity of targets to detect targets (Fadili et al. 2010). It includes low-rank and sparse representation for frame sequences and single image frames. Multiple algorithms for different backgrounds have used convex or non-convex functions to approximate low-rank and sparsity models. Researchers have considered small targets as sparse components and background clutters as low-rank components. Based on this theory, a small target estimation method using the robust principal component analysis (RPCA) is for small target image detection (Wang and Qin 2015). RPCA is optimizing the low-rank and sparsity matrix. The optimal decomposition of RPCA can be achieved through the iterative threshold (IT), accelerated proximal gradient (APG), and augmented lagrange method (ALM) or alternative direction method of multipliers (ADMM). The RPCA algorithm weights the singular values of the low-rank matrix and sparse matrix, which improves the accuracy of the detection result. However, the algorithm is biased and its approximation result cannot be optimal (Zhou and Tao 2011). The Godec algorithm considers the characteristics of complex background noise and decomposes the image into low-rank sparse components. It has improved robustness in noisy environments. It is heavily reliant on the image rank and sparsity threshold, resulting in poor stability. According to the characteristic that the

foreground will be distributed in local areas, a low-rank and structured sparse decomposition algorithm is proposed (Gao et al. 2013). The method has the potential to improve adaptability to noisy environments, but it has a lower computational efficiency. The author constructs an IPI model to achieve a better low-rank and sparse representation (Ye et al. 2015). It can be used in a single frame with a high detection rate. The original IPI method suffers from the disadvantages of salient edge residuals and sparse noise. Many methods focus on solving the IR small target detection based on the IPI model under a complex environment. The article (Li et al. 2015) comprehensively considers the motion characteristics of small targets and uses the motion matrix to weight the sparse matrix. Under the same false alarms, it can improve the sparsity of moving targets and the algorithm's detection rate. However, the weighted matrix contains a large number of parameters, making it difficult to adjust multiple parameters to achieve a unified optimization effect. The article (He et al. 2015) uses a joint spatiotemporal sparse recovery method to distinguish target atoms from background spatiotemporal atoms, which is not highly adaptable to complex backgrounds. The author (Wang et al. 2017) proposes to detect weak and small targets by sparse representation in small target images and eliminate the noise matrix. It has comprehensively considered the adaptability to noise background, but the real-time performance is not good. The paper proposes to use total variation regularization and principal component tracking methods to solve the weak target detection ability with non-uniform and non-smooth scenes, which could better adapt to complex background environments with high temporal and spatial complexity (Peng et al. 2012). The article has verified that RASL (Robust alignment by sparse and low-rank decomposition) can adapt to complex environments and has a relatively faster turnaround time (Wang et al. 2017). However, it requires the manual selection of target regions in video sequences. The author utilizes the weighted nuclear norm model in the low-rank and sparse representation based on the IPI model, which could keep the details of targets and increase the detection rate (Gu et al. 2017). It improves the image recovery effect. Recently, an image-patch tensor (IPT) model makes full use of the structural information between pixels (Zhang et al. 2019). The small target detection problem is transformed into an optimization problem for separating the low-rank and sparse parts of the tensor. The method detects the small target precisely and can keep a higher signal-to-clutter ratio (SCR). The L_p norm minimization of singular values in the existing IPI methods replaces the nuclear norm minimization (NNM) for a complex background. The re-weighted IPI model with total variance (TV) suppresses the noise and preserves the strong edges in the background with a post-processing filter (Wan et al. 2022).

Based on the above research on the IPI model, this paper presents a sparse representation of noisy infrared images based on the WIPI model. We combine multi-scale local contrast with post-processing for small target detection in an actual single infrared image frame. An improved weighted nuclear norm optimization algorithm completes low-rank decomposition with robust principle component analysis (RPCA). It effectively suppresses the background faults and improves the detection rate. Compared to traditional spatial filtering and low-rank model detection, it is more robust against complex backgrounds with high noise. Thus, we can largely suppress the background and improve signal-to-noise ratio gain (SCRG) in real IR images.

Methods workflow

There aren't many data sets for infrared image sequences at the moment. Sometimes it is hard to meet general requirements by relying solely on the sequences obtained by experimental groups. Infrared detectors can only obtain corresponding images for preliminary verification of detection methods in specific environments. An IPI model is to detect small targets in a single infrared image, which can achieve reliable detection of small and medium-sized targets with small amounts of data sets. Following that, various improvements and applications have been made to this model for a variety of applications. They further improve the efficiency of the original algorithm. Subsequently, the author presented a weighted IPI (WIPI) detection method with the effects of clutters and noise. Each target block is assigned a different weight in order to obtain a more accurate estimate. Based on the above research, this paper proposes an infrared small target detection algorithm based on the WIPI model. Our method achieves the fusion of WIPI and local non-uniformity contrast enhancement post-processing. It is more adaptable to the complex environment containing high Gaussian noise. The detection strategy is depicted in Figure 1. The flowchart, as you can see, is divided into four sections. First, we construct the matrix with a low-rank background and sparse target based on the IPI model. Second, the

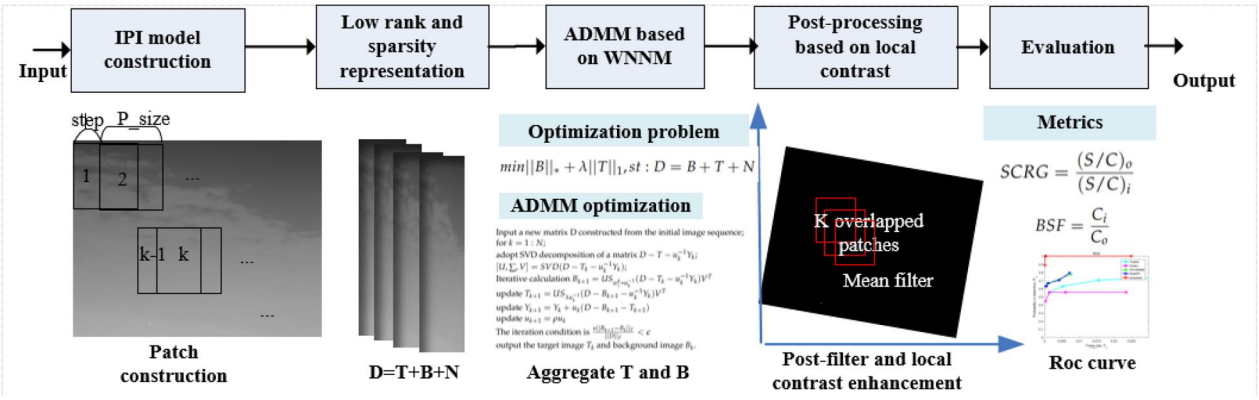

Figure 1. Infrared small target detection with WIPI mode based on local contrast post-processing.

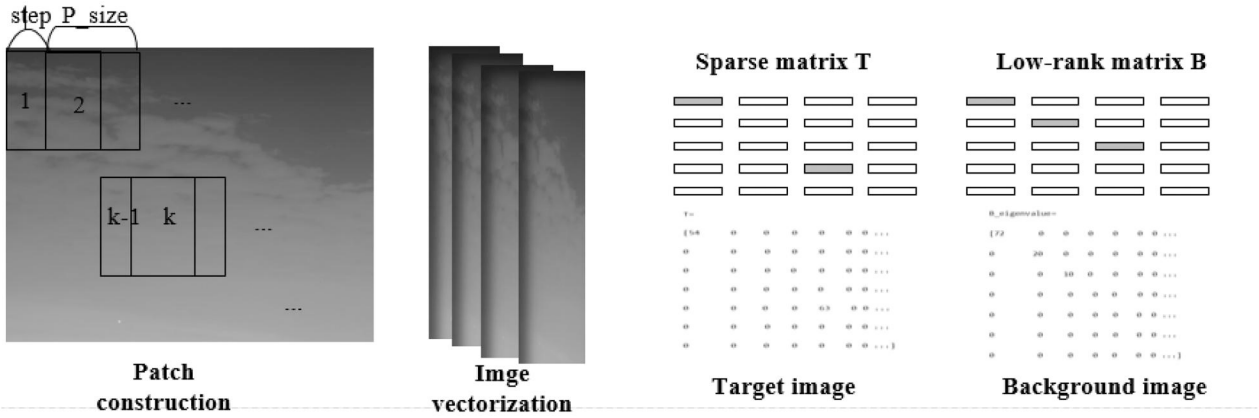

Figure 2. The construction diagram of IPI image.

weighted nuclear-norm minimization is adopted for the background matrix, which remains the strong background edge and textures. In the meantime, the target matrix is more sparse when vectorization is done properly. Third, the local contrast post-processing is applied to the recovered target image. It is useful for strengthening the target and suppressing the residual background. Finally, we could use the adaptive segment threshold to achieve the target and evaluate the detection results among some metrics. We put our method to the test in a large number of real-world IR images. It demonstrates that our method has the ability to improve the target detection and background suppression.

Principle and construction of IPI model

The IPI model is based on two assumptions. First, infrared images have nonlocal-correlations. Local blocks are used to create a new matrix. It is a low-rank matrix. Second, the target only occupies a few pixels and presents a sparse property. As a result, using low rank and sparsity representation, it is possible to achieve the separation of the background and the target. Infrared image sequences can be described as the accumulation of targets, backgrounds, and noise. A typical low-rank and sparse matrix can be considered to be the composition of an image frame. A low-rank matrix can be used to represent the background, which has a strong correlation. A sparse matrix represents the target, which can range from a few to dozens of pixel points. Noise is mainly composed of Gaussian noise, whose l_2 norm is less than a specified minimum value, which represents the cost function.

The IPI matrix structure is shown in the following Figure 2. Select the packet window size $50 * 50, 80 * 80, 100 * 100$, and set the number of sliding steps 5, 8, 10, 20. Slide the window from the head of the image frame until the end of the image frame. The new window obtained by each sliding is used as a new column of the newly constructed matrix. We ultimately achieve an N column new matrix. The matrix includes a low-rank background portion and a sparse target.

The construction diagram of IPI image is a vectorization of the original image. We could try our best to keep the structure information by selecting the proper parameters, such as packet size and sliding step.

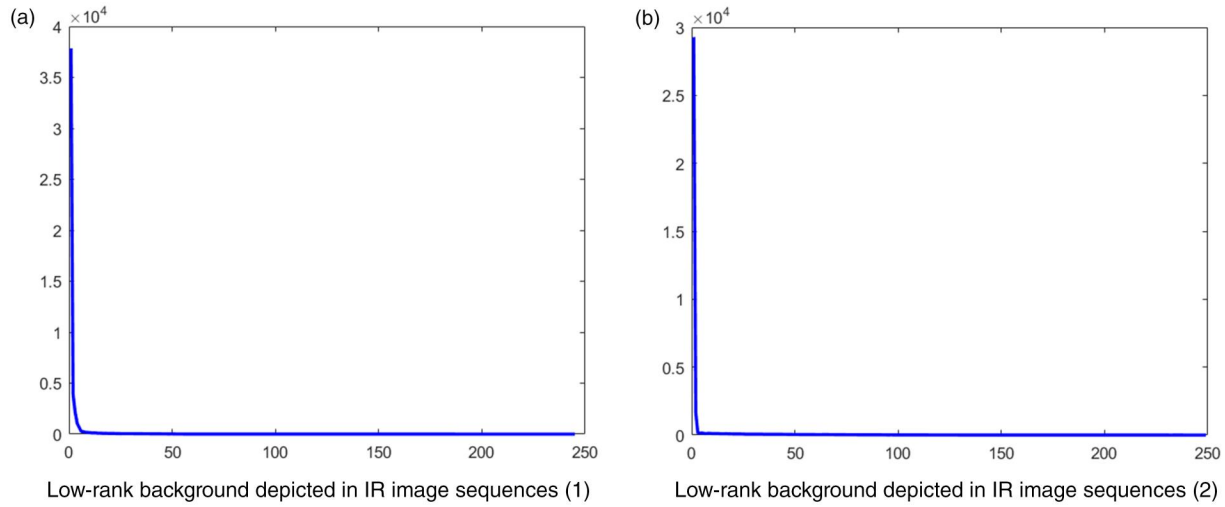

Figure 3. Rank results in IR image sequences.

Low rank and sparse representation

The small target detection is thought to be a low rank and sparse decomposition. The original low rank representation problem is NP hard. As a result, we must make an approximate representation of the expression. The robust principal component analysis (RPCA) can achieve convex optimization approximation of the original NP problem. The minimization of the low rank space and sparsity is replaced by minimizing the sum of the low rank matrix nuclear norm and the sparse matrix l_1 norm. The problem can be described as follows in (1).

$$\min||B||_* + \lambda||T||_1, st : D = B + T + N \tag{1}$$

D represents the initial input image. B is the background of the low-rank portion and M stands as the target image of the sparse portion. λ is used to balance the low-rank and sparse portions. It represents the iteration contraction step size, which determines the number of iterations to converge. The low-rank and sparse decomposition of a matrix is to solve the B and T matrices corresponding to the smallest of the above equations. The optimization function can be solved using an alterative threshold (IT) algorithm, an accelerated proximal gradient (APG) algorithm, and an alternative direction method of multiplier (ADMM). The B and T matrices can be finally solved to obtain the target image and background image by setting a small penalty term. In the end, we locate the small target in the target image. The low-rank background is depicted in Figure 3.

ADMM algorithm based on weighted nuclear norm model

The nuclear norm of the infrared image background corresponds to the eigenvalue of the background matrix. The larger the eigenvalue of the background matrix, the more image information is contained. As a result, using the weighted nuclear norm, the image texture information can be enhanced further to complete the target and background segmentation. The original problem can be transformed into the following unconstrained problem by introducing a Lagrange multiplier Y. The equation is displayed in (2).

$$L(B,T,Y,u) = argmin||B||_{w,*} + \lambda||T||_1 + < Y, L - T - B > + u\frac{||D-B-T||_F^2}{2}, st : L = B + T + N \tag{2}$$

To solve the problem, we define the soft threshold value as in (2).

$$S_\epsilon(X) = \begin{cases} X - \epsilon & (X \geq \epsilon) \\ X + \epsilon & (X \leq \epsilon) \end{cases} \tag{3}$$

The traditional nuclear norm model treats all eigenvalues equally and ignores the difference in their meanings.The larger eigenvalue represents the main component, which contains details and textures. The iterative shrinkage needs to use the different factor for the different eigenvalue. Inspired by the article (He et al. 2015), the weighted nuclear norm model is used in the optimization by (4).

$$w_i^k = \frac{C}{\delta_i(B^{k-1}) + \epsilon} \tag{4}$$

w_i^k is the ith weight of the kth iteration. $\delta_i(B^{k-1})$ stands for the ith singular value of the matrix B, which is achieved by the $(i-1)$th iteration. C is a constant.

The alternating direction multiplier method (ADMM) based on the WIPI model can be described as follows.

- Input a new matrix D constructed from the initial image sequence;
- for $k = 1 : N$;
- adopt SVD decomposition of a matrix $D - T - u_k^{-1}Y_k$;
- $[U, \sum, V] = SVD(D - T_k - u_k^{-1}Y_k)$;
- Iterative calculation $B_{k+1} = US_{w_i^k * u_k^{-1}}(D - T_k - u_k^{-1}Y_k)\ V^T$
- Update $T_{k+1} = US_{\lambda u_k^{-1}}(D - B_{k+1} - u_k^{-1}Y_k)V^T$
- Update $Y_{k+1} = Y_k + u_k(D - B_{k+1} - T_{k+1})$
- Update $u_{k+1} = \rho u_k$
- The iteration condition is $\frac{u||B_{k+1}-B_k||_F}{||D||_F} < \tau$
- Output the target image T_k and background image B_k.

By alternately updating the target matrix and background matrix, the function could gradually iterates to convergence. We have set small penalty so that Gaussian noise is suppressed. Finally, the small target image and background image are obtained. Compared with the nuclear norm model, we could achieve better details for the original image.

Post-processing based on multi-scale local contrast

RPCA is widely used in denoising and target detection due to the robustness of principal component analysis under complex noisy environments. Specific Gaussian noise standard deviations are designed for actual infrared image sequences. It makes it easier to determine the adaptability of detection methods in noisy environments. We consider the detection scenarios of small infrared targets against the background of bright buildings on the ground and undulating clouds in the sky. Then we perform block sparse representation on infrared images with low noise and high noise separately. After decomposition by ADMM, sparse target and low-rank background images are obtained respectively.

The gray of the overlapping regions is obtained by using a mean value operation on the overlapping regions of the target image. Averaging the overlapping regions of the background image can achieve better robustness to high noise. The mean filter is used to recover the overlapped block, which is resistant to noise interference. Larger contrast can be obtained in the target image by performing multi-scale local intra-block consistency and non-consistency contrast analysis on the restored target image.

The mean value of cell elements in the central area is m_T, and the mean value of cell elements in the four directions around the central area is respectively m_{Bi} $(i = 1, 2, 3, 4)$. We design the local contrast measurement (LCM) between the center cell as in (5).

$$d(T, Bi) = m_T - m_{Bi}d_i = d(T, Bi) * d(T, B(i+4)) \tag{5}$$

The center cell gray is replaced by (6).

$$C(x_i, y_j) = min_{i=1}^4 d_i. \tag{6}$$

The window sliding to the target area can increase the brightness of the target. If sliding to the background area, the method suppresses the background intensity. When the target scale is not clear, multi-scale feature map can obtain the maximum response with multi-scale. After the saliency feature map is obtained by preprocessing, the local enhanced contrast is calculated. It has better robustness against a variety of different types of non-cooperative small targets by designing a variety of scales, and it also plays a better role in suppressing Gaussian noise that only occupies a single pixel. Multi-scale contrast is expressed as (7).

$$\max C_n^l = C_x(x_i, y_j)^l. \tag{7}$$

Small targets can be enhanced under a certain range of intensity noise. Then we perform adaptive threshold segmentation, which allows us to accurately obtain the target. We integrate the alternating direction multiplier method and add a post-processing operation. It uses the mean value to obtain pixel restoration of overlapping region blocks. At the same time, the multi-scale local contrast of the post processing method can play a better role in enhancing the target and suppressing the background through joint operations. Compared with traditional spatial filtering and local low-rank sparse decomposition, it can adapt to complex background with high noise. At last, it has a higher detection rate under the same false alarm rate.

Evaluation

SCRG, BSF, and the ROC curve, which are quantitative indexes based on the subject standard, are the most common detection evaluation metrics. The

SCRG is shown in (8). It is defined by the SCR of the output image and the SCR of the original input image (Ji 2007).

$$SCRG = \frac{(S/C)_o}{(S/C)_i} \tag{8}$$

S is the difference between the entire image and the small target. C is the standard deviation of the whole image. $()_i$ and $()_o$ stand the parameters of input images and output ones.

BSF is defined by the standard deviation ratio of input images and output images. It is shown in (9).

$$BSF = \frac{C_i}{C_o} \tag{9}$$

The detection rate and false alarm rate are the two components of the ROC curve. The detection rate is defined as the ratio of the number of real target pixels detected to the number of target pixels in (10).

$$P_d = \frac{TP}{T}. \tag{10}$$

TP is the number of real targets pixels detected. T is the number of real target pixels.

The false alarm rate is defined as the ratio of the number of false target pixels detected to the total number of false target pixels, as shown in 1(1) (Ruitao Lu et al. 2020).

$$P_f = \frac{FP}{F} \tag{11}$$

FP is the number of false target pixels detected. F is the number of false target pixels.

The larger SCRG and BSF indicate better target enhancement and background suppression effect. The larger the area of the ROC curve, the better the detection effect.

Experimental results and comparisons

Real IR image attained from the IR detector system

Our work is based on the real IR detection system which has tracked fast-moving airplanes. We use the IR cool mid-wave detector *CMS*6055 to develop the outdoor experiment. It occupies the $3 \sim 5um$ mid-wave infrared band and produces $640 * 512$ resolution image sequences. The single pixel size is $15um$. The target is less than $3 * 3$ pixels according to the detection distance.

By building an outfield test platform, multiple image sequences were taken with the sky and ground buildings as the background. Gaussian noise processing is used to obtain infrared images with different noise intensities based on the real-time captured images. Compared with the traditional Top-hat algorithm, Godec model algorithm, RPCA algorithm based on IPI (Gu et al. 2017), and ReWIPI (Guo et al. 2018), we could evaluate the advantages of infrared target detection methods based on IPI model post-processing fusion mechanism in suppressing background effects and target enhancement. The sequences have special characteristics in the Table 1.

The size of all images is $m * n$. All method parameters are listed in the Table 2.

Simulation and analysis

The simulation uses a personal computer with an Intel core i7 CPU and 16 GB of RAM and performs

Table 1. Features of image sequences.

Feature	a	b	c	e	f	g
Image number	20	20	20	20	20	20
Target	1 flight	1 flight	1 flight	1 flight	1 flight	1 flight
Target size	2*2	2*2	3*3	2*2	2*2	3*3
Noise std	/	/	/	10	10	10
Backgound	heavy cloud	highlight buildings	complex buildings	heavy cloud	highlight buildings	complex buildings

Table 2. Comparison parameters with different detection methods.

Method	Parameters
Top-hat	template size 3*3
Godec	$patchsize = 80 * 80, slidingstep = 10, rank = 6, card = 3.1 * 10^5$
IPI + WNNM	$patchsize = 80 * 80, slidingstep = 10, \tau = 10^{-6}, \lambda = 1/\sqrt{\min(m,n)}$
ReWIPI	$patchsize = 80 * 80, slidingstep = 10, \tau = 10^{-6}, \lambda = 1/\sqrt{\min(m,n)}, k\_\max = 1, \epsilon\_R = 0.04, \epsilon\_T = 0.04$
Proposed	$patchsize = 80 * 80, slidingstep = 10, \tau = 10^{-6}, \lambda = 1/\sqrt{(\min(m,n))}, \epsilon = 10^{-6}, C = 2.82, u = 0.9, l = 4$

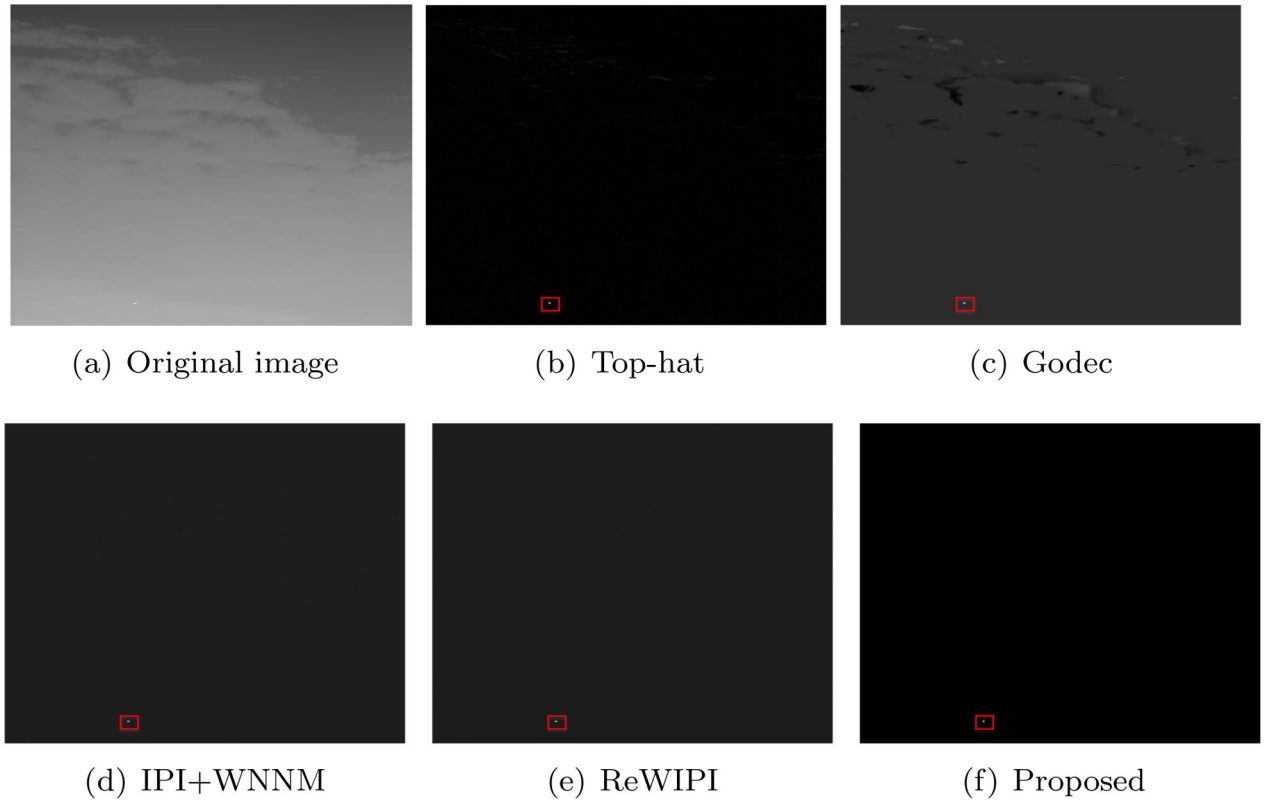

Figure 4. Detection results for different methods in image (a).

simulation on the MATLAB R2016a simulation platform. We input different complexity infrared image frame sequences (a), (b), (c), and noised image frames (e), (f), (g). Then we could simulate the detection effects of the traditional Top-hat algorithm, Godec model algorithm, WNNM model based on IPI, ReWIPI, and WIPI model based on local contrast post-processing in complex background image sequences. At the same time, we compared the detection effects of algorithms in image frames with different noise std (Figures 4–12).

The captured infrared small target sequence images are shown in Figure 4(a), Figure 8(a), and Figure 12(a). The background in Figure 4(a) includes large clouds with a continuous background and sparse target characteristics. In Figure 8(a), highlighted buildings are included in the image background. The background is consistent and has a strong correlation. However, the correlation between the target pixel points and their adjacent regions is weak, despite the fact that they are sparse. The intensity of the target is low, and it is easily submerged. In Figure 12(a), the image contains a complex architectural background, with some bright and strong brightness clumps. The target exhibits sparsity. It is prone to false alarms. The image (a), image (b), and Image (c) separately add a certain standard deviation of Gaussian noise to form a noisy image as the image (e), image (f), and image (g). When we add std10 noise, the target could hardly be prominent and submerged in noise in the image (e), image (f) and image (g). The results and 3D Mesh display of the original image sequence and the noisy image sequence are shown in Figure 4, Figure 5, Figure 6, Figure 7, Figure 8, Figure 9, Figure 10, Figure 11, Figure 12, Figure 13, Figure 14, and Figure 15 with different detection methods.

From the above detection images, it can be seen that the fusion post-processing detection algorithm has good detection effects in various types of images. The results are displayed with a high level of visual contrast, and the background is completely suppressed. It has a good detection and comparison effect under noisy environment.

The SCRG of image (a), image (b), image (c), noised image (e), noised image (f), noised image (g) are shown in Table 3 with different methods. The BSF of the image sequences are shown in the Table 4.

Infrared image sequences obtained higher SCRG and BSF through the fusion detection method from above tables. It demonstrates that the algorithm's

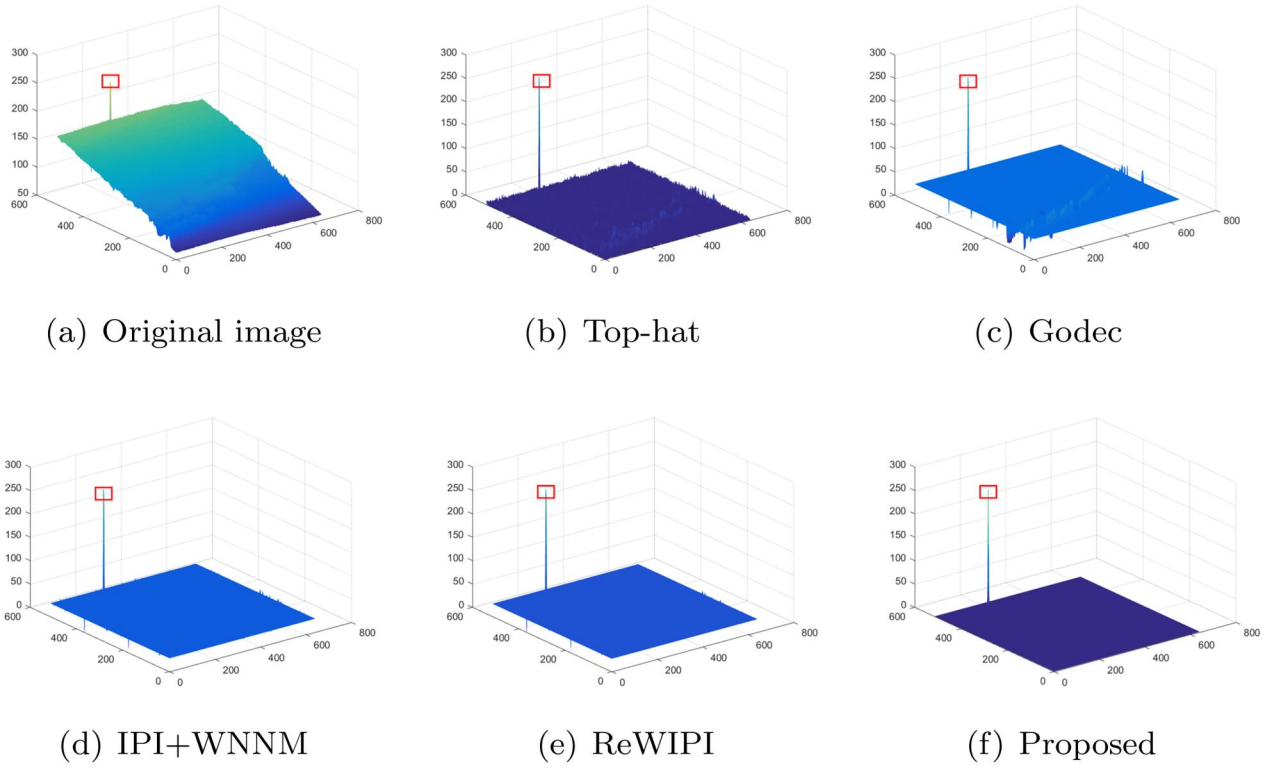

Figure 5. 3D mesh results for different methods in image (a).

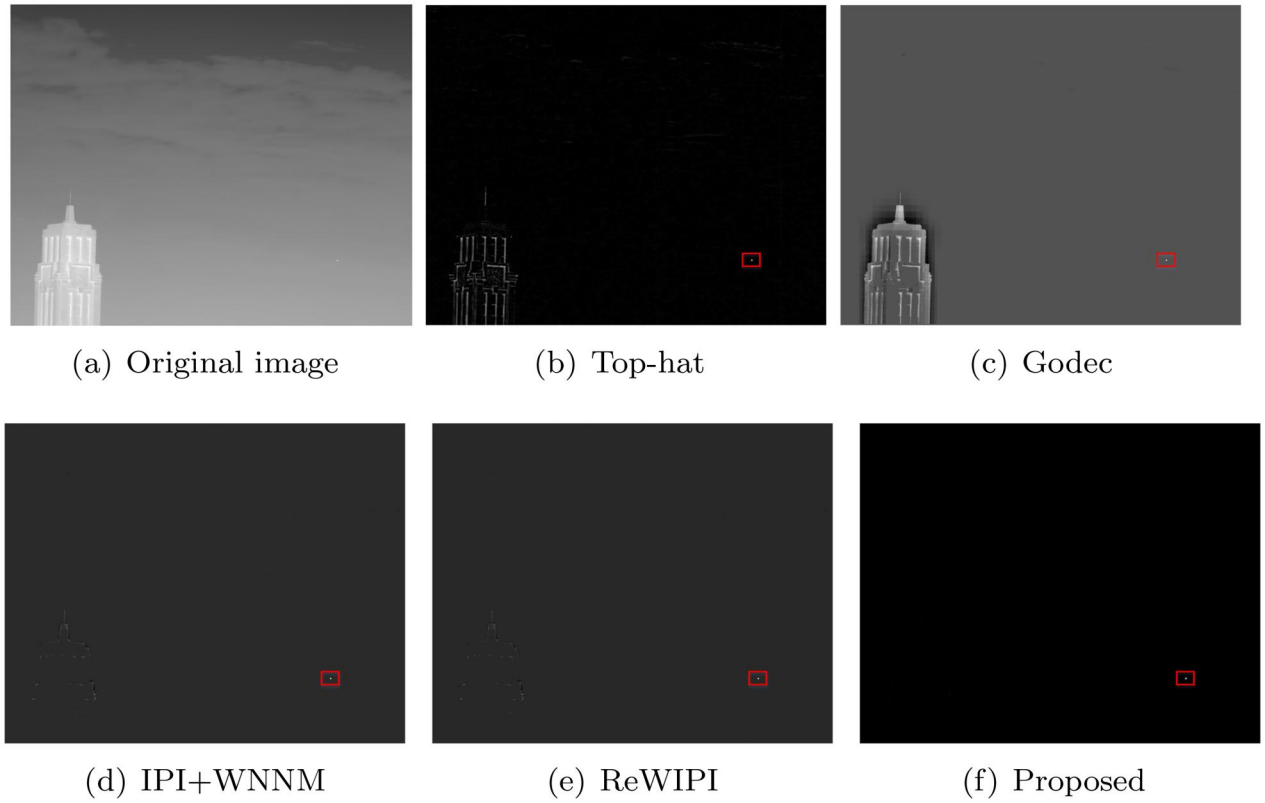

Figure 6. Detection results for different methods in image (b).

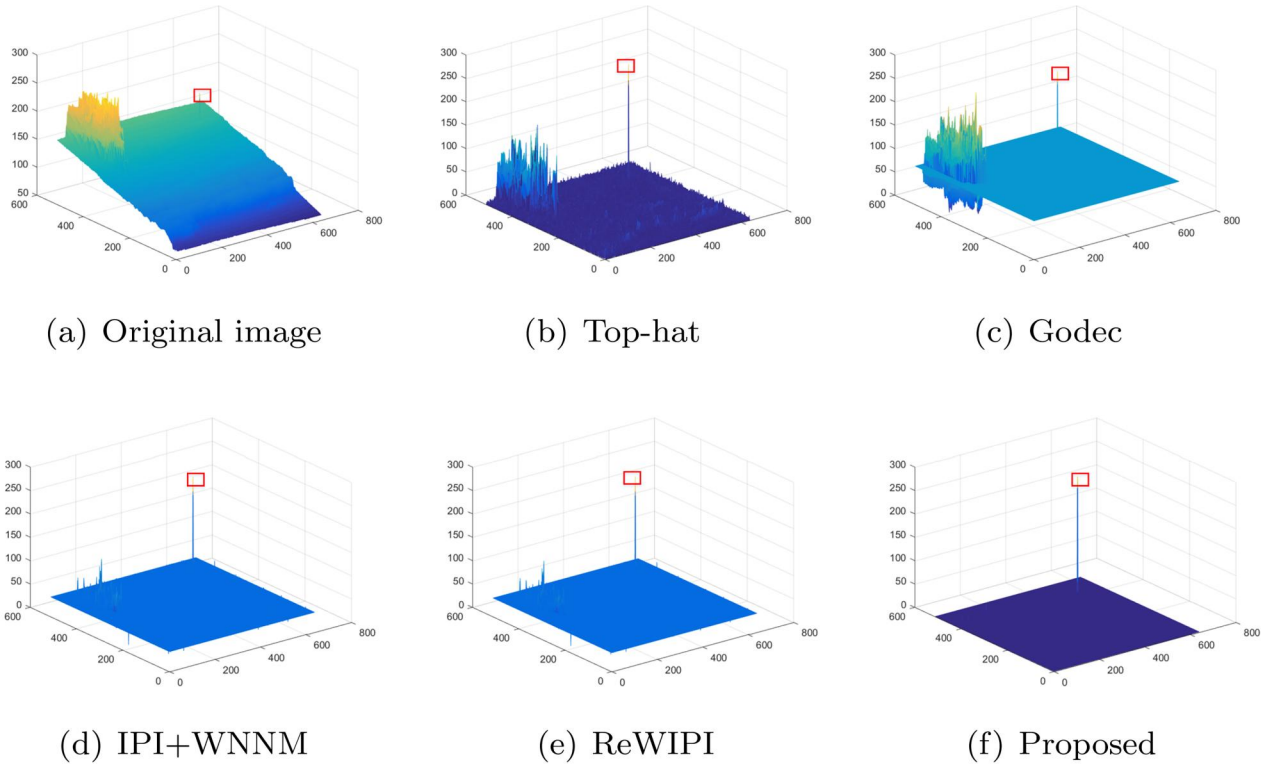

Figure 7. 3D mesh results for different methods in image (b).

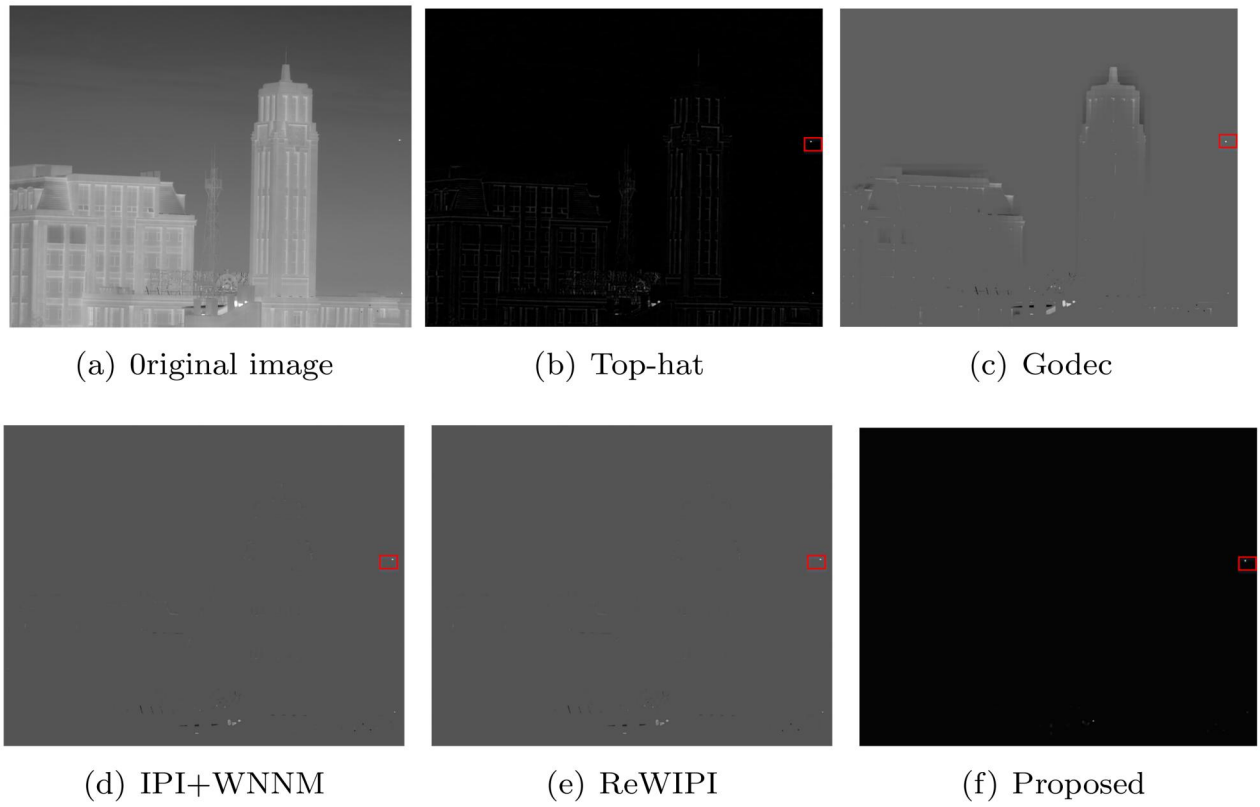

Figure 8. Detection results for different methods in image (c).

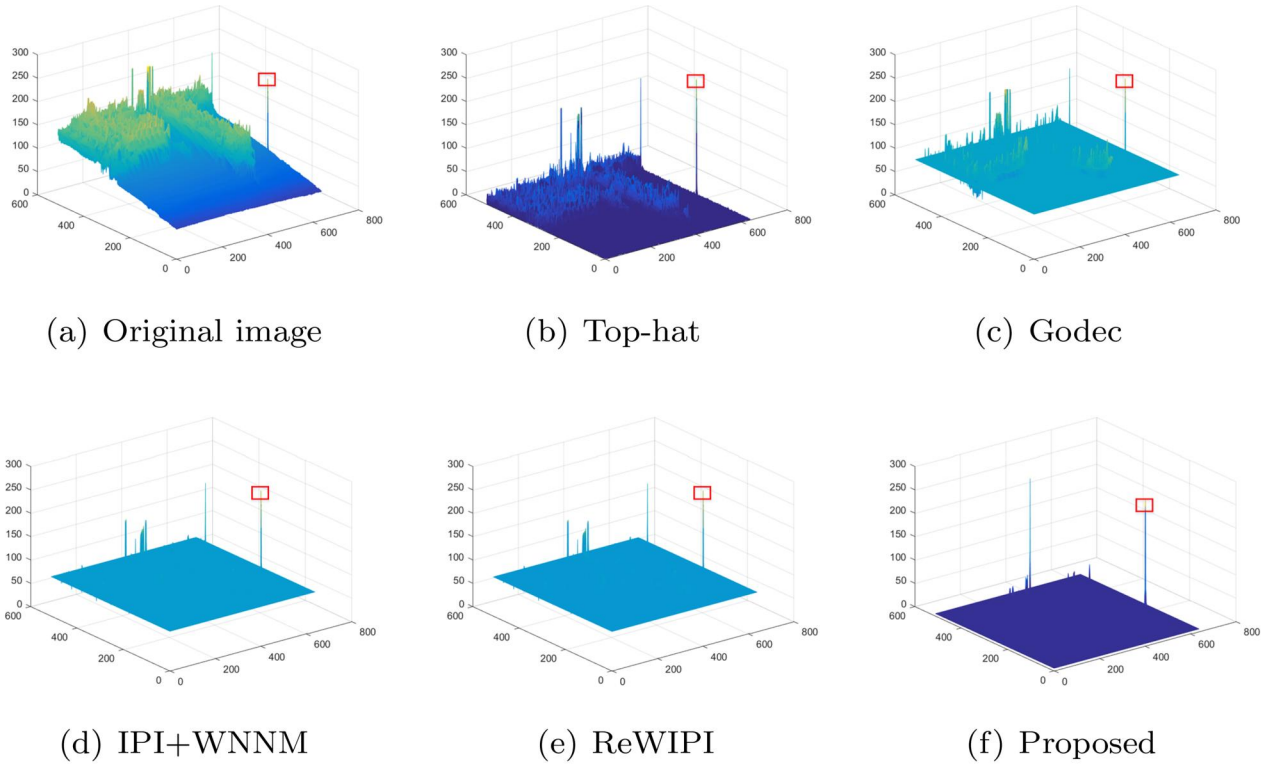

Figure 9. 3D mesh results for different methods in image (c).

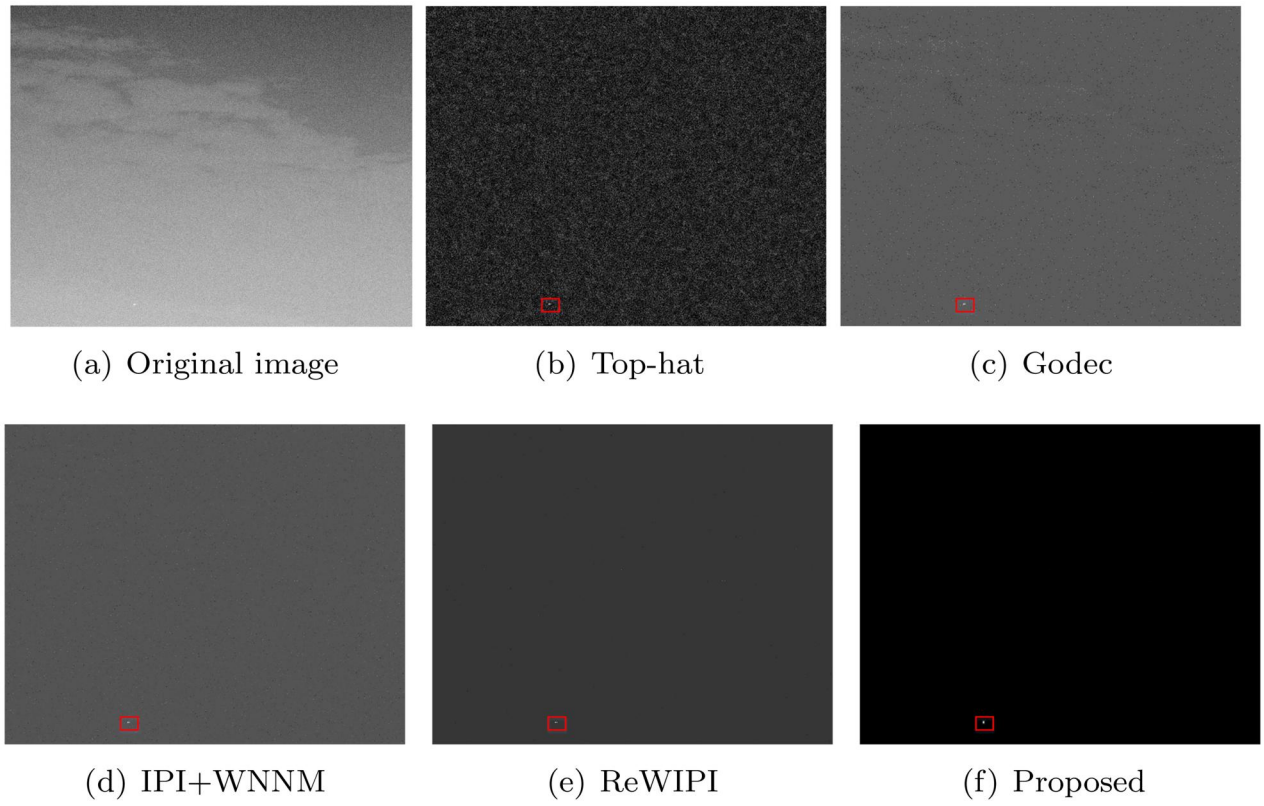

Figure 10. Detection results for different methods in noise image (e).

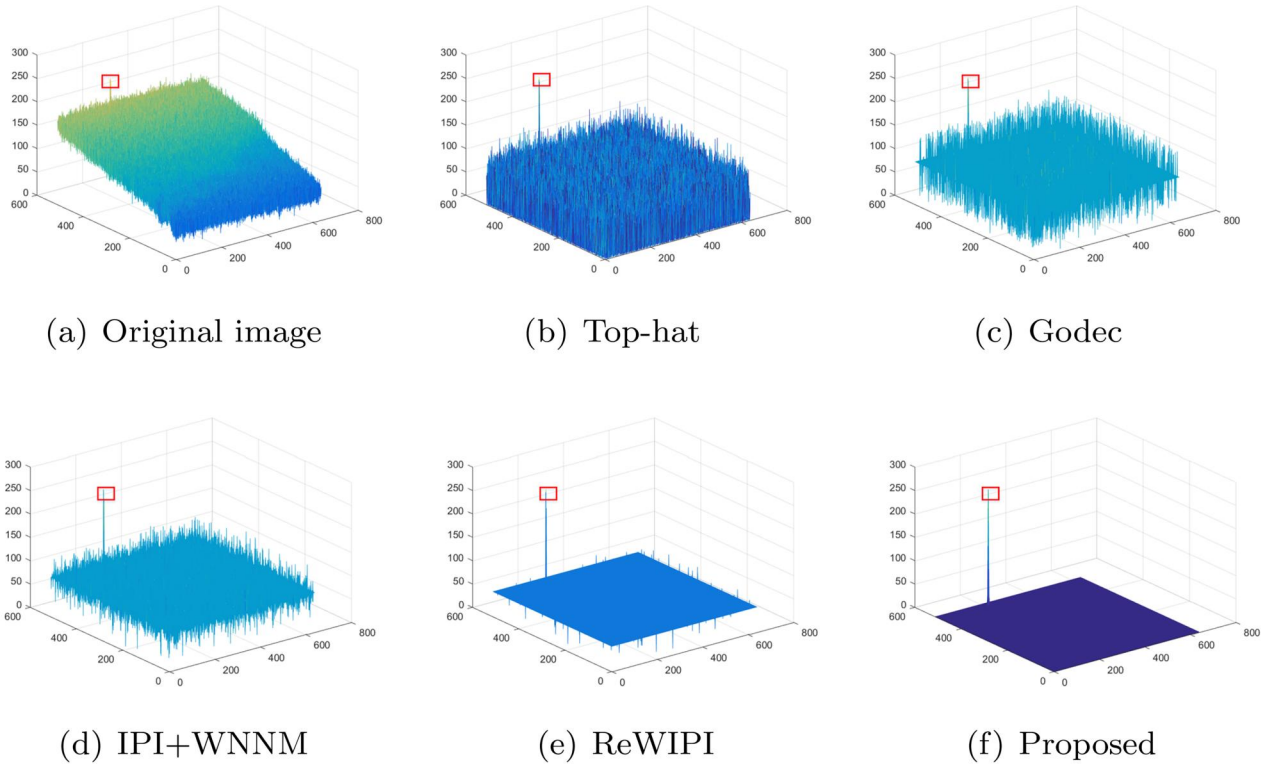

Figure 11. 3D mesh results for different methods in noise image (e).

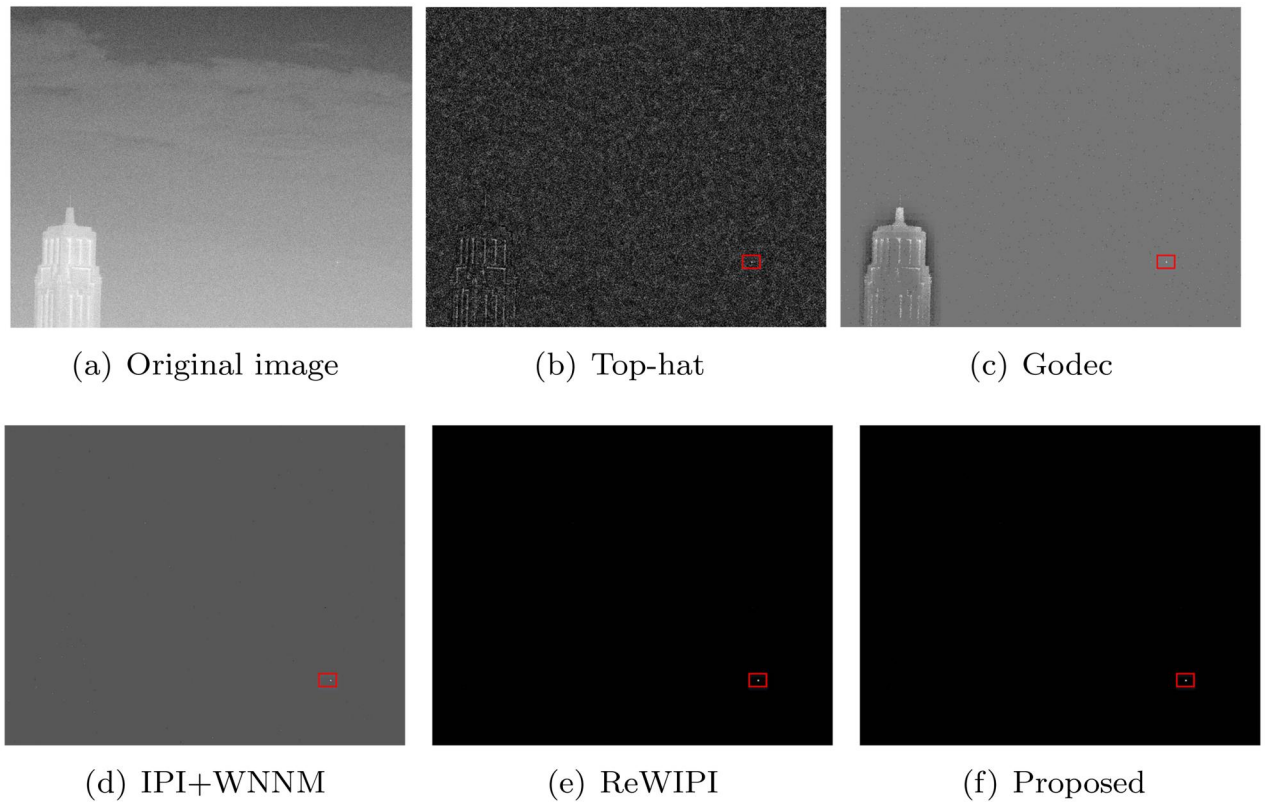

Figure 12. Detection results for different methods in noise image (f).

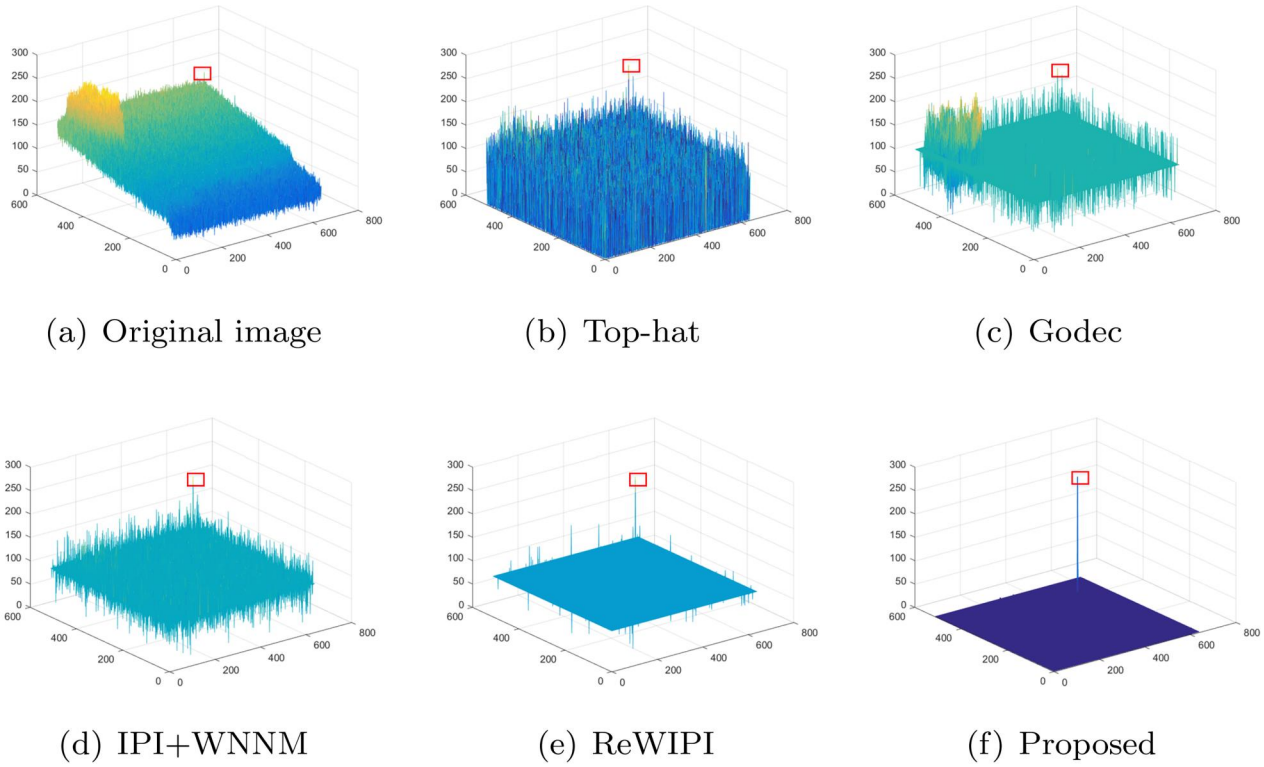

(a) Original image (b) Top-hat (c) Godec

(d) IPI+WNNM (e) ReWIPI (f) Proposed

Figure 13. 3D mesh results for different methods in noise image (g).

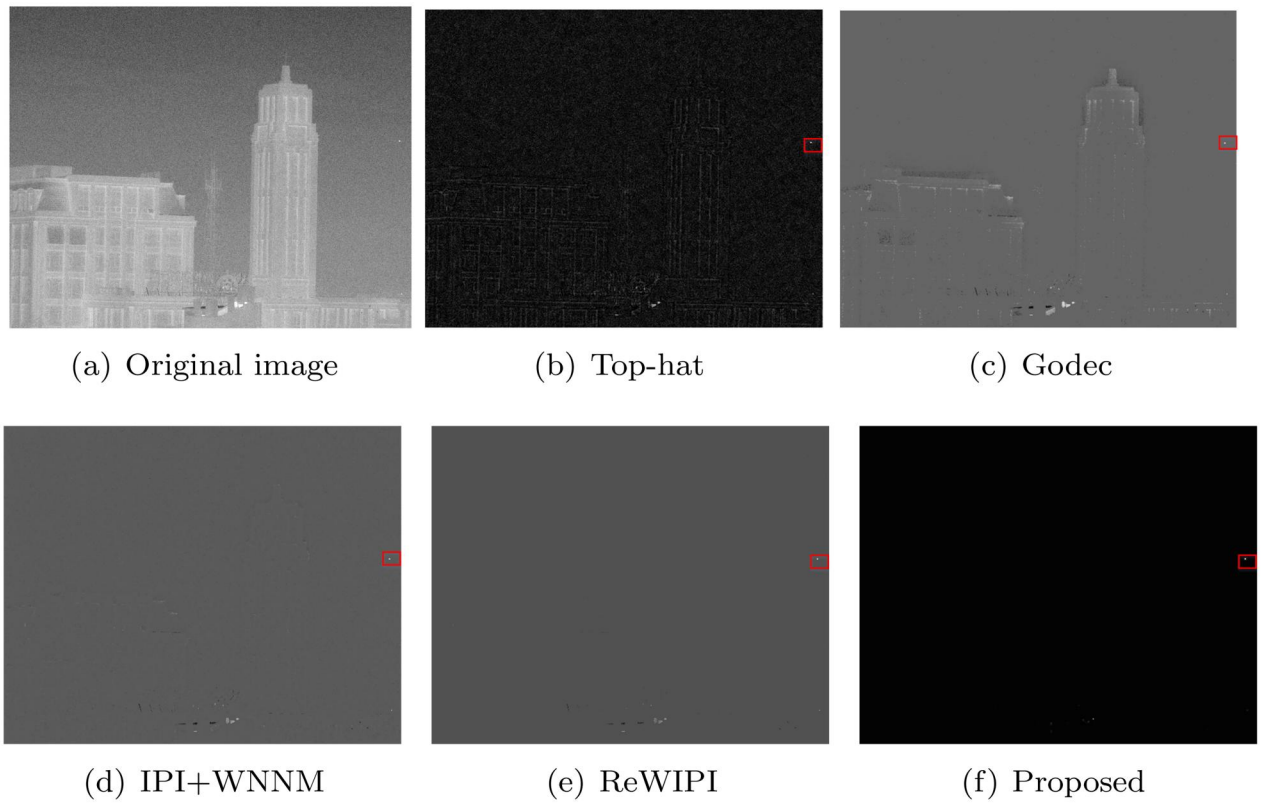

(a) Original image (b) Top-hat (c) Godec

(d) IPI+WNNM (e) ReWIPI (f) Proposed

Figure 14. Detection results for different methods in noise image (g).

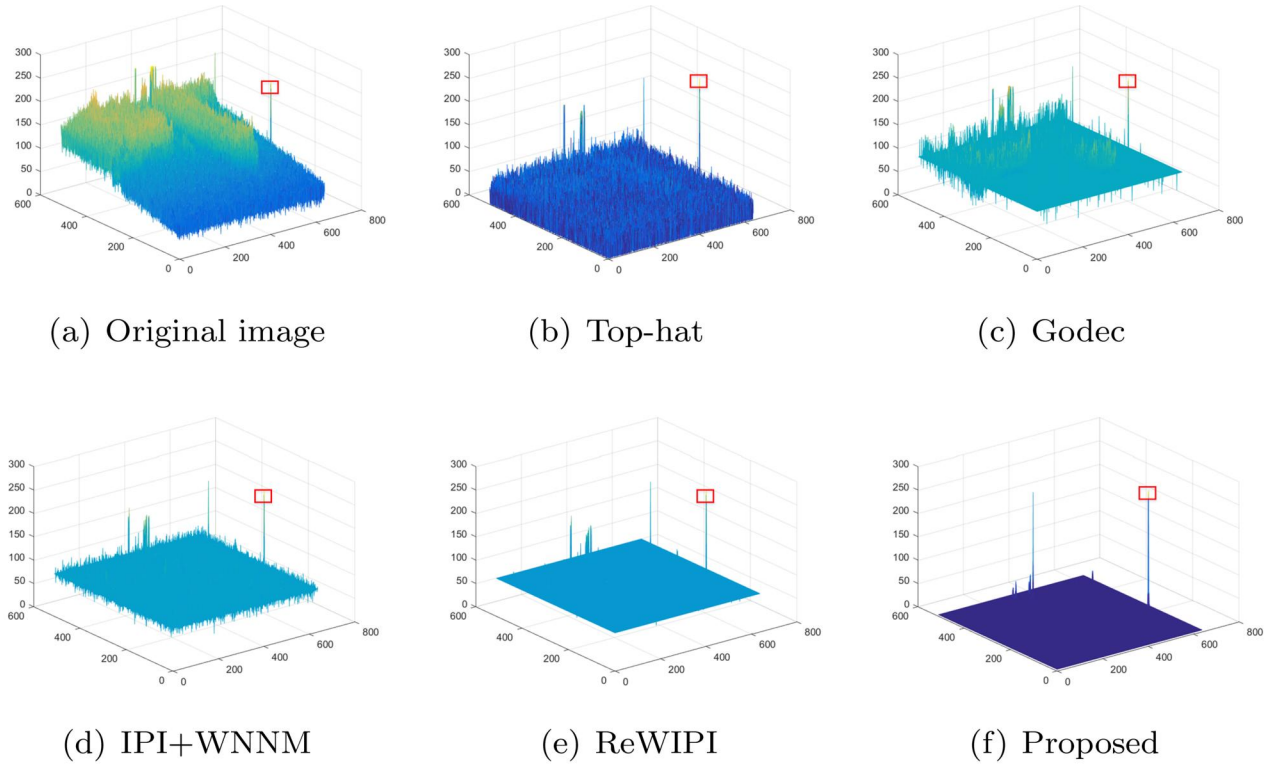

Figure 15. 3D mesh results for different methods in noise image (g).

Table 3. Comparison results of SCRG with different detection methods.

Method	a	b	c	e	f	g
Top-hat	26.704	13.484	9.689	2.083	2.321	4.266
Godec	19.964	7.067	9.587	6.029	6.145	8.755
IPI + WNNM	105.21	75.552	24.417	9.186	9.571	14.514
ReWIPI	128.184	85.185	25.565	53.845	43.595	31.735
Proposed	3825.343	832.543	91.451	664.329	673.488	126.088

Table 4. Comparison results of BSF with different detection methods.

Method	a	b	c	e	f	g
Top-hat	13.87	4.656	5.37	1.238	1.044	2.415
Godec	12.429	3.903	8.399	4.739	4.429	7.574
IPI + WNNM	61.16	30.97	19.963	6.919	5.89	11.714
ReWIPI	74.186	34.543	20.845	34.381	24.1291	24.195
Proposed	1979.645	285.258	55.156	335.058	246.77	66.425

detection performance has improved. It still has better SCRG and BSF in noisy images, which indicates that the fusion algorithm has good adaptability to the environment.

We utilize an WIPI model detection algorithm that fuses local contrast post-processing to detect small targets in actual image sequences. It can improve the detection effect compared to traditional spatial filtering and low-rank sparse decomposition algorithms.

Finally, the ROC curve has been completed. The abscissa is the false positive rate. And the Y-axis is the true positive rate. The ROC curves of the above detection methods are shown in the following Figure.16. The ROC curve of the proposed strategy in this paper shows the good performance in actual infrared image sequences including original images and high noise images. Our method is prior to Tophat, Godec, IPI + WNNM, ReWIPI. The results indicate that the proposed algorithm is robust to our IR image sequences. Above all, our method can achieve better SCRG and BSF with clear details and textures. Compared with other common used methods based on the IPI model, we could gain better ROC results. And our method is more appropriate for a high-noise environment. It demonstrates some stability under complex backgrounds. It is capable of detecting small targets more stably and accurately. Our method is a fusion detection based on the WIPI model. The computation complexity is higher with the low rank and sparsity decomposition because the SVD decomposition needs cubic power computation of the matrix row or columns. At the same time, the iteration computation with ADMM is time-cost. We need to make some simplified calculations and do our best to improve the timeliness.

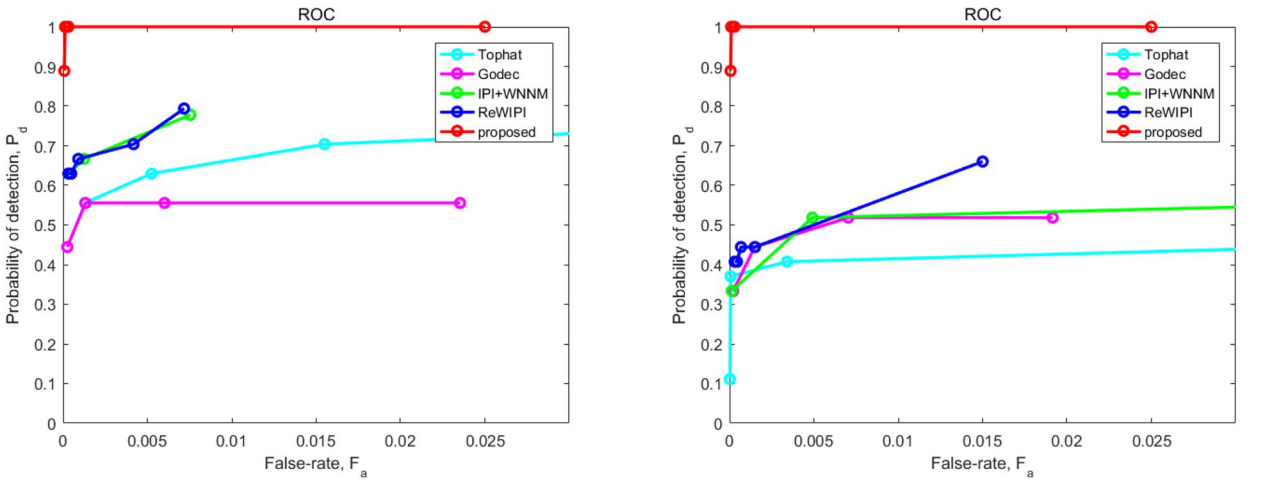

Figure 16. ROC results for different methods in IR image sequences.

Conclusions

The low-rank sparse decomposition based on the IPI model is fused with the local contrast post-processing. Through simulation verification and analysis, the method can better suppress the background in infrared images with noise. It has good adaptability to complex backgrounds, especially in a high-noise environment.

The WIPI originates from the IPI theory.The matrix is created by the patch-searching strategy, which is made up of the target, the background, and the noise. A WNNM model is shrinking every eigenvalue with different factors. The larger eigenvalue stands for a more principal component, which should shrink less when the optimization is implemented. The method remains strong edges and uneven details. The WIPI model for IR small target detection based on multi-scale local contrast post-processing has suppressed the highlight noise and some residual edges. Adopting the ADMM optimization method, the convex problem is solved with a globally optimum solution. The post-processing includes average filter and multi-scale contrast enhancement. It is more resistant to noise and a variety of target sizes. The test images in a real environment have verified our method achieves the highest PSNR and BSF among all images under different backgrounds. Simultaneously, we are unaffected by the noise environment. Our next task will be to strike a balance between computation complexity and recovery accuracy.

Acknowledgments

The authors would like to thank Innovation Academy for Microsatellites of Chinese Academy of Sciences. It is a best research platform which provides much support for us.

Disclosure statement

No potential conflict of interest was reported by the author(s).

Funding

This research was funded by Youth Innovation Promition Association of the Chinese Academy of Sciences under Grant[No. 2022296].

ORCID

Juan Chen http://orcid.org/0000-0001-7450-957X
Lin Qiu http://orcid.org/0000-0002-3407-488X
Wai-Hung Ip http://orcid.org/0000-0001-6609-0713
Kai-Leung Yung http://orcid.org/0000-0001-9091-6140

References

Cao, L., Zhang, X., and Wang, Z. 2021. "Arbitrary-oriented object detection on high resolution images based on differentiable architecture search." *Canadian Journal of Remote Sensing*, Vol. 47 (No. 5): pp. 719–730. doi:10.1080/07038992.2021.1955666.

Chen, C.L.P., Li, H., Wei, Y., Xia, T., and Tang, Y.Y. 2014. "A Local Contrast Method for Small Infrared Target Detection." *IEEE Transactions on Geoscience and Remote Sensing*, Vol. 52 (No. 1): pp. 574–581. doi:10.1109/TGRS.2013.2242477.

Cheng, M., Xu, C., Wang, J., Zhang, W., Zhou, Y., and Zhang, J. 2022. "MicroCrack-Net: A Deep Neural Network With Outline Profile-Guided Feature Augmentation and Attention-Based Multi-Scale Fusion for MicroCrack Detection of Tantalum Capacitors." *IEEE Transactions on Aerospace and Electronic Systems*, Vol. 58 (No. 6): pp. 5141–5152. doi:10.1109/TAES.2022.3181117.

Fadili, M.J., Starck, J.-L., Bobin, J., and Moudden, Y. 2010. "Image decomposition and separation using sparse

representations: an overview." *Proceedings of the IEEE*, Vol. 98 (No. 6): pp. 983–994. doi:10.1109/JPROC.2009.2024776.

Gao, C., Meng, D., Yang, Y., Wang, Y., Zhou, X., and Hauptmann, A.G. 2013. "Infrared patch-image model for small target detection in a single image." *IEEE Transactions on Image Processing*, Vol. 22 (No. 12): pp. 4996–5009. doi:10.1109/TIP.2013.2281420.

Gu, S., Xie, Q., Meng, D., Zuo, W., Feng, X., and Zhang, L. 2017. "Weighted nuclear norm minimization and its applications to low level vision." *International Journal of Computer Vision*, Vol. 121 (No. 2): pp. 183–208. doi:10.1007/s11263-016-0930-5.

Guo, J., Wu, Y., and Dai, Y. 2018. "Small target detection based on reweighted infrared patch-image model." *IET Image Processing*, Vol. 12 (No. 1): pp. 70–79. doi:10.1049/iet-ipr.2017.0353.

Han, J., Ma, Y., Zhou, B., Fan, F., Liang, K., and Fang, Y. 2014. "A robust infrared small target detection algorithm based on human visual system." *IEEE Transactions on Geoscience and Remote Sensing Letters*, Vol. 11 (No. 12): pp. 2168–2172.

Han, J., Liang, K., Zhou, B., Zhu, X., Zhao, J., and Zhao, L. 2018. "Infrared small target detection utilizing the multiscale relative local contrast measure." *IEEE Geoscience and Remote Sensing Letters*, Vol. 15 (No. 4): pp. 612–616. doi:10.1109/LGRS.2018.2790909.

He, YJie., Li, M., Zhang, JLi., and An, Q. 2015. "Small infrared target detection based on low-rank and sparse representation." *Infrared Physics & Technology*, Vol. 68: pp. 98–109. Voldoi:10.1016/j.infrared.2014.10.022.

Ji, Q. 2007. The Research on Dim Small Target Detection in Infrared Image Sequences. PHD thesis. Harbin: Harbin Engineering University.

Jia, L., Shaojuan, L., and Yingjuan, Z. 2019. "Infrared Image Background Suppression Based On Multiscale Generalized Fuzzy Operator." *Semiconductor Opto electronics*, Vol. 1 (No. 40(01)).

Li, Z., Hou, Q., Fu, H., Dai, Z., Yang, L., Jin, G., and Li, R. 2015. "Infrared small moving target detection algorithm based on joint spatio-temporal sparse recovery." *Infrared Physics & Technology*, Vol. 69 (No. 9): pp. 44–52. (doi:10.1016/j.infrared.2015.01.008.

Lin, Z. 2012. *Research on Weak Target Track-Before-Detect Technologies for Space-based Infrared Image*. Changsha: National University of Defense Technology.

Lu, R., Yang, X., Li, W., Fan, J., Li, D., and Jing, X. 2020. "Robust infrared small target detection via multidirectional derivative-based weighted contrast measure." *IEEE Geoscience and Remote Sensing Letters*, Vol. 19: pp. 1–5. doi:10.1109/LGRS.2020.3026546.

Lv, Y., Li, M. 2022. "Ship Detection in SAR Images via Cross-Attention Mechanism." *Canadian Journal of Remote Sensing*, Vol.48 (No.6): pp. 764–778.

Mu, X., Feng, L., and He, J. 2021. "A fast recursive LRX algorithm with extended morphology profile for hyperspectral anomaly detection." *Canadian Journal of Remote Sensing*, Vol. 47 (No. 5): pp. 731–748.

Peng, Y., Ganesh, A., Wright, J., Xu, W., and Ma, Y. 2012. "RASL: Robust alignment by sparse and low-rank decomposition for linearly correlated images." *IEEE Transactions on Pattern Analysis and Machine Intelligence*, Vol. 34 (No. 11): pp. 2233–2246. doi:10.1109/TPAMI.2011.282.

Qin, Y., and Li, B. 2016. "Effective infrared small target detection utilizing a novel local contrast method." *IEEE Geoscience and Remote Sensing Letters*, Vol. 13 (No. 12): pp. 1890–1894. doi:10.1109/LGRS.2016.2616416.

Ruhan, A., Mu, X., Feng, L., and He, J. 2021. "A fast recursive LRX algorithm with extended morphology profile for hyperspectral anomaly detection." *Canadian Journal of Remote Sensing*, Vol. 47: (No. 5): pp. 731–748. doi:10.1080/07038992.2021.1959307.

Shi, Y., Wei, Y., Yao, H., Pan, D., and Xiao G. 2017. "High boost based mutiscale local contrast measure for infrared small target detection." *IEEE Geoscience and Remote Sensing Letters*, Vol. 15 (No. 1): pp. 33–37.

Wan, M., Gu, G., Xu, Y., Qian, W., Ren, K., and Chen, Q. 2022. "Total variation-based interframe infrared patch-image model for small target detection." *IEEE Geoscience and Remote Sensing Letters*, Vol. 19: pp. 1–5. doi:10.1109/LGRS.2021.3126772.

Wang, J., Zhao, S., Xu, C., Zhang, J., and Zhong, R. 2023a. "Brain-inspired interpretable network pruning for smart vision-based defect detection equipment." *IEEE Transactions on Industrial Informatics*, Vol. 19 (No. 2): pp. 1666–1673. doi:10.1109/TII.2022.3188349.

Wang, J., Gao, P., Zhang, J., Lu, C., and Shen, B. 2023b. "Knowledge augmented broad learning system for computer vision based mixed-type defect detection in semiconductor manufacturing." *Robotics and Computer-Integrated Manufacturing*, Vol. 81: pp. 102513. Voldoi:10.1016/j.rcim.2022.102513.

Wang, C., and Qin, S. 2015. "Adaptive detection method of infrared small target based on target-background separation via robust principle component analysis." *Infrared Physics & Technology*, Vol. 69: pp. 123–135. doi:10.1016/j.infrared.2015.01.017.

Wang, X., Peng, Z., Kong, D., Zhang, P., and He, Y. 2017. "Infrared dim target detection based on total variation regularization and principal component pursuit." *Image and Vision Computing*, Vol. 63: pp. 1–9. doi:10.1016/j.imavis.2017.04.002.

Wang, H., Lou, J., Zhang, C., *et al.* 2017. "Infrared small dim target detection based on weighted nuclear norm minimization." *2017 IEEE 7th Annual International Conference on CYBER Technology in Automation, Control, and Intelligent Systems (CYBER). IEEE*. pp. 388–393.

Wei, Y., You, X., and Li, H. 2016. "Multiscale patch-based contrast measure for small target detection." *Pattern Recognition*, Vol. 58 (No. C): pp. 216–226. doi:10.1016/j.patcog.2016.04.002.

Wu, B. 2008. *Research on the Detection of Small and Dim Targets in Infrared Images*. Xian: Xidian University.

Yilong, L., and Li, M. 2022. "Ship Detection in SAR Images via Cross-Attention Mechanism." *Canadian Journal of Remote Sensing*, Vol. 48 (No. 6): pp. 764–778. doi:10.1080/07038992.2022.2118109.

Ye, X., Yang, J., Sun, X., Li, K., Hou, C., and Wang, Y. 2015. "Foreground–background separation from video

clips via motion-assisted matrix restoration." *IEEE Transactions on Circuits and Systems for Video Technology*, Vol. 25 (No. 11): pp. 1721–1734. doi:10.1109/TCSVT.2015.2392491.

Zhang, X., Ding, Q., Luo, H., Hui, B., Chang, Z., and Zhang, J. 2019. "Infrared small target detection based on an image-patch tensor model." *Infrared Physics & Technology*, Vol. 99: pp. 55–63. doi:10.1016/j.infrared.2019.03.009.

Zhou, T., and Tao, D. 2011. "Godec: Randomized low-rank & sparse matrix decomposition in noisy case." *Proceedings of the 28th International Conference on Machine Learning*, *ICML* **2011**.